

# Optical identification using physical unclonable functions [Invited]

PANTEA NADIMI GOKI,<sup>1,2,\*</sup> STELLA CIVELLI,<sup>2,3</sup> EMANUELE PARENTE,<sup>2</sup> ROBERTO CALDELLI,<sup>4,5</sup> THOMAS TEFERI MULUGETA,<sup>2</sup> NICOLA SAMBO,<sup>2</sup> MARCO SECONDINI,<sup>2</sup> LUCA POTÌ<sup>1,5</sup>

<sup>1</sup>Photonic Networks and Technologies Laboratory, CNIT, Via G. Moruzzi 1, 56124, Pisa, Italy

<sup>2</sup>TeCIP Institute, Scuola Superiore Sant'Anna, Via G. Moruzzi 1, 56124, Pisa, Italy

<sup>3</sup>CNR-IEIIT, Via Caruso 16, 56122, Pisa, Italy

<sup>4</sup>CNIT Florence Research Unit, Viale Morgagni 65, 50134, Florence, Italy

<sup>5</sup>Universitas Mercatorum, Piazza Mattei 10, 00186, Roma, Italy

\*Corresponding author: [pantea.nadimigoki@santannapisa.it](mailto:pantea.nadimigoki@santannapisa.it)

Received XX Month XXXX; revised XX Month, XXXX; accepted XX Month XXXX; posted XX Month XXXX (Doc. ID XXXXX); published XX Month XXXX

---

**In this work, the concept of optical identification (OI) is introduced for the first time. The OI assigns an optical fingerprint and the corresponding digital signature to each sub-system of the network and estimates its reliability in different measures. We highlight the large potential applications of OI as a physical layer approach for security, identification, authentication, and monitoring purposes. To identify most of the sub-systems of a network, we propose to use the Rayleigh backscattering pattern, which is an optical physical unclonable function and allows to achieve OI with a simple procedure and without additional devices. The application of OI to fiber and path identification in a network, and to the authentication of the users in a quantum key distribution system are described.**

---

## 1. INTRODUCTION

The rapid growth of global communication networks around the globe requires optimal network security protocols.

Each layer of the open systems interconnection (OSI), which describes how different layers communicate in a network, contributes to the overall security of the network, which includes secure communication, authentication, identification, and monitoring. Figure 1 depicts the security protocols that can be applied to the layers of the OSI, briefly described below. The application layer, which is the layer with which most of the users interact, may include end-to-end cryptography, e.g., Outlook, Skype, and WhatsApp messages are encrypted to be recognized just by users. Also, the presentation and session layers, which are responsible for syntax processing and creating communication channels between devices, respectively, may profit from data cryptography. The transport layer, which is responsible for the transmission of data across network connections, may use secure sockets layer (SSL) or transport layer security (TLS) protocols that include authentication between parties, data integrity, and digital signature. The network layer, which handles the routing of the data, is responsible for security at the network level and uses functions such as

packet authentication, cryptography, and integrity, e.g., Internet protocol security (IPsec). The data link layer uses admission controls to check and guarantee the proposed connection, for example, wireless systems developed Wi-Fi protected access (WPA). Concerning the physical layer, usually, security is not implemented because establishing optimal security protocols at this level is still an open worldwide problem. Although the upper layers are liable to security and confidentiality, implementing a security protocol on the physical layer could significantly enhance the network's security. Potential attacks that target the physical layer are included tampering (which introduces fake nodes), jamming (which introduces harmful signals in the network), side-channel attacks (when the adversary gets physical access to the device), physical infrastructure attacks, and eavesdropping. Hence, physical layer security (PLS) is a crucial element that can enhance the overall security of the networks. To establish PLS several methods have been proposed and studied. The very first technique based on information theoretic characterizations of secrecy for PLS is the Wyner technique which is defined by the wiretap channel model [1]. The Wyner technique limits the information to an eavesdropper by using the channel capacity difference between a target receiver and an eavesdropper, defining positive secrecy capacity only if the target receiver has better signal-to-noise ratio (SNR) than the eavesdropper, which makes this technique unsecured. An adversary

with high-performance devices can receive higher SNR than the target receiver. The eavesdropper attack may be neutralized, by transmitting the artificial noise to reduce its channel capacity, only if the attacker's position is known [2]. Since then, various research has been done in this area, and most of them that guarantee security is based on suited encoding and complicated modulation schemes [3,4].

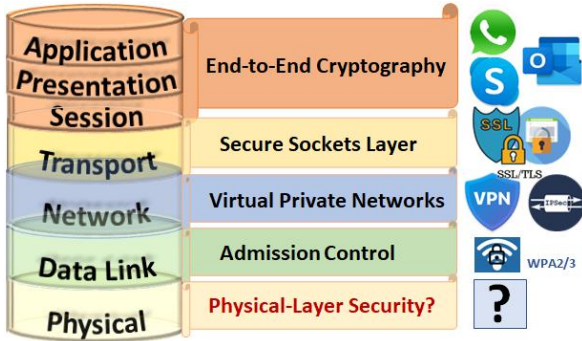


Fig. 1. Security along Open system interconnection (OSI) levels. The target of our proposed method in this paper is to implement a novel (ID) technique for physical layer security.

The PLS techniques based on computational cryptography rely on computational hardness, but are vulnerable to digital attacks. For instance, PLS based on asymmetric key cryptography is susceptible to machine learning attacks [5]. Quantum key distribution (QKD) [6,7] provides intrinsic security, but (i) is not cost-effective, (ii) is hard to be implemented, and (iii) relies on user authentication usually performed with classical techniques. Also, the PLS based on keys generated by digital signal processing (DSP) [8] is vulnerable to digital attacks. Recently, an approach based on optical steganography was proposed to hide messages below the noise level [9,10]. However, this technique cannot detect the presence of an eavesdropper and is vulnerable to adversaries who know the technique [11,12]. PLS-based optical chaos communication [13,14] requires high-level synchronization between the transmitter and the receiver [15] and its security can be broken in some scenarios [16].

A new approach to PLS is based on the material's physical features, defined by physical unclonable functions (PUFs), in which a physical device provides unique output for a given input [17]. The security of this method relies on the intrinsic unclonability of the PUF [18-20], and, therefore, is able to overcome the disadvantages of computational cryptography. Optical PUFs (OPUFs), PUF defined in the optical domain, have been recently studied [21-24]. Even though OPUFs have been investigated for secure cryptography key generation, they were never employed in a real system as a practical security solution [25].

Despite all the effort aforementioned to implement PLS, it is still an open problem. Indeed, optical fibers, which constitute the larger part of the physical layer, are distributed around the globe and are vulnerable to adversarial attacks, whose capabilities are growing day by day thanks to the use of high-performance devices or exploiting intensive machine learning algorithms. In this paper we propose a novel method to ensure network security: the optical identification (OI). The OI is based on the Rayleigh backscattering pattern (RBP) extracted from an optical fiber, which is a strong OPUF [26]. The proposed method can be used for communication security, authentication, identification, and monitoring, both in point-to-point communication and optical networks.

This manuscript is organized as follows. In Section 2, we introduce the concept of optical identification and its security validation. In Section 3, we introduce the concept of optical physical unclonable function, and we describe the Rayleigh backscattering. Next, Section 4 describes some

potential applications of the OI concepts, and Section 5 provides some examples. Finally, Section 6 draws conclusions.

## 2. OPTICAL IDENTIFICATION

### A. Concept

Not only humans but also physical elements have their own fingerprints. In general, the fingerprint (equivalently, signature) of a device, system, or sub-system, denoted below as ID, is related to its physical characteristics and caused by imperfections in the manufacturing process. In this manuscript, we propose to exploit the inherent characteristics of fiber network systems to produce a fingerprint to be used for security purposes, a concept that has not been used in communication systems and networks. We refer to this concept as optical identification (OI) and we briefly describe it in the following.

A point-to-point scenario, sketched in Figure 2(a), is made of three sub-systems: transmitter, channel, and receiver. Let us denote the signatures of these three sub-systems as  $ID_{TX}$ ,  $ID_{Ch}$ , and  $ID_{RX}$ , respectively. In this case, three possible security approaches may be envisaged: (i) the transmitter reads  $ID_{Ch}$  and  $ID_{RX}$  to be sure that the information passes the expected channel and reaches the expected receiver, (ii) the receiver reads  $ID_{TX}$  and  $ID_{Ch}$  to be sure who is the sender and which is the physical path, (iii) the transmitter reads  $ID_{RX}$  and the receiver acquires  $ID_{TX}$  so that both know to whom they are talking (they can also acquire  $ID_{Ch}$  to check the path).

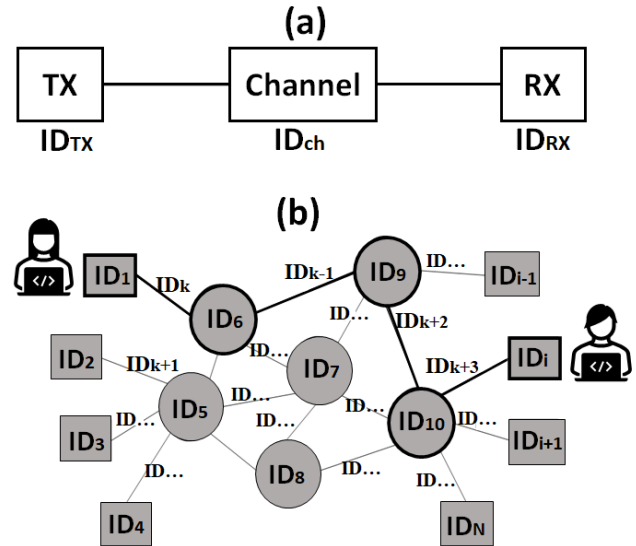


Fig 2. (a) A point-to-point communications system. (b) Example of network architecture.

In a network scenario with  $N$  sub-systems, sketched in Figure 2(b), each sub-system may be identified by its signature, labeled as  $ID_i$  where  $1 \leq i \leq N$  represents the  $i$ -th sub-system. In an optical network, sub-systems may include transceivers, optical fibers, optical nodes, filters, optical cross-connects, reconfigurable optical add/drop multiplexers, etc.

The ID of each sub-system, both in a point-to-point scenario or the network scenario, can be generated and stored in a database. Each sub-system is identified by comparing its ID with the corresponding stored copy, and correct identification is characterized by probability  $p_i$ . In a network scenario, any sub-system may be able to identify another sub-system in the network and, eventually, validate the whole path. Let us consider the bold path in Figure 2(b). If the sub-system with  $ID_1$  is able

to evaluate the probability of each path and these paths are independent, each sub-system can be independently interrogated, and the probability of the whole path becomes:

$$p = \prod_{i \in \{path\}} p_i \quad (1)$$

The above model allows us not only to validate each sub-system and the path but also to identify whether any changes occurred in the path and where. However, the acquisition of the signature of the sub-system is not independent. Consequently, a more complex model based on the specific technique used for identification must be developed.

## B. Security validation

The ID of each sub-system can be represented by a vector of bits, the digital signature. How this digital signature is obtained depends on the specific implementation, and some examples are given in the next sections.

It is important to underline that, even if the physical signature is unclonable, its digital representation loses this property. As a consequence, is essential to be able to assess the accuracy and strength of a signature generation method. Below, we describe how to perform the identification of a binary signature, and how to assess its strength.

Let us assume there are two users U and V, in a point-to-point communication, each with their digital signature with  $N$  bits. To compare two signatures, we use the inter-Hamming distance (HD), which counts the number of different bits among the two signatures.

Assuming that the bits of each signature are independent and identically distributed and that  $p$  is the probability of having different bits in the two IDs, the HD of two signatures is distributed as a binomial distribution with  $N$  trials and mean value  $Np$ . This means that when two IDs are independently generated,  $p = 0.5$  and the mean is  $N/2$ . Conversely, when two IDs are not dissimilar (which happens when they represent the same sub-system) a few bits should be flipped to obtain one from the other, i.e.,  $p$  and the HDs are small. Consequently, the decision rule is: if HD is below a certain threshold  $t$ , we assume that the two IDs represent the same user; conversely, if the HD is larger than  $t$ , we assume that the IDs belong to different users.

This concept is illustrated in Figure 3, which reports the probability of the HD between the IDs of the users U and V with the stored ID of the user U. The figure shows that the mean of the HD for U, denoted as  $M_U$ , is much lower than the one for V, denoted as  $M_V$ . The threshold  $t$  can be defined as

$$t = \gamma M_V + (1 - \gamma) M_U \quad (2)$$

where  $0 \leq \gamma \leq 1$ .

The success or failure of the procedure depends not only on intrinsic physical limitations and inaccuracies (e.g., the amount of noise in the RBP acquisition) but also on the post-processing method i.e., signature definition and decision rule (e.g., the number of bits). The procedure fails when a false negative or a false positive occurs. On the one hand, a false negative ‘‘U rejected’’ occurs when U is the user, but the procedure fails, and he is rejected (the HD is larger than  $t$ ). This is a matter of identification, which can be partly mitigated by repeating the identification protocol several times. On the other hand, a false positive ‘‘V accepted’’ occurs when the user is V (different from U), but the procedure fails, and V is identified as U (the HD is smaller than  $t$ ). This is a matter of security and authentication. In general, while it is desirable to minimize both the probability of false negative and false positive, one can tailor  $t$  to the system requirements: if  $t$  decreases, the security improves (the probability of false positive decreases) at the expense of identification capabilities (the probability of false negative increases). The probability of failure (the sum of the probability of false positive and false negative) can be evaluated (i) estimating by simulations the mean

of the HD of the right user  $M_U$  (two signatures of U) and of the wrong user  $M_V$  (the signature of U and the signature of V) (ii) considering the two binomial distributions with  $N$  trial, and probability of success  $M_U/N$  and  $M_V/N$ , respectively, and (iii) estimating the probability of false positive as:

$$\sum_{k=0}^{HD} \binom{n}{k} \left(\frac{M_V}{N}\right)^k \left(1 - \frac{M_V}{N}\right)^{N-k} \quad (3)$$

and the probability of a false negative as:

$$\sum_{k=HD}^{\infty} \binom{n}{k} \left(\frac{M_U}{N}\right)^k \left(1 - \frac{M_U}{N}\right)^{N-k} \quad (4)$$

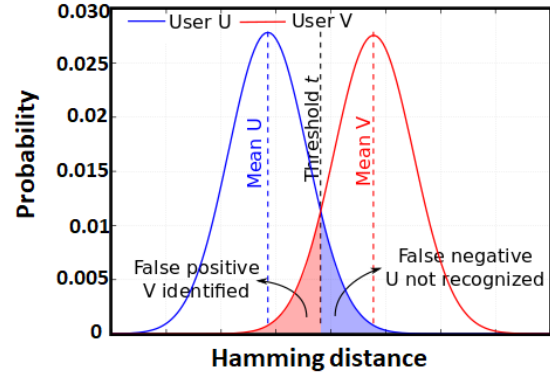


Fig. 3. Probability of HD of two users. The false positive and false negative regions are highlighted, depending on the decision rule.

Depending on the scenario and type of signature, it is straightforward to use quick response (QR) codes to represent signatures (simply binary matrices). In this case, the robustness of the method also can be evaluated by considering the inner HD and the intra-HD, as in [27]. These two are useful to demonstrate the robustness of the signature against a digital forecasting attack and to demonstrate ID reproducibility. Inner HD is the HD of a pair of 1D segments in the QR code that should not be too smaller or bigger than half of the size of the segment length to be robust against digital attacks.

Intra-HD is the HD of several repeated measures of the same sub-system, and should be low to indicate the reproducibility of the ID.

## 3. OPTICAL PUF

### A. Concept

A physical unclonable function (PUF) is, by definition, a function that, under specific circumstances and for a given input (referred to as *challenge*) provides a unique output (*response*) that results to be unclonable [28]. The uniqueness of the signature is a physical characteristic of the PUF, usually due to the imperfections of the manufacturing process. A PUF can be generated by physical objects, like the communication and network sub-systems, e.g., sensors, integrated circuits, and hardware in general. In a nutshell, PUFs provide a signature, or fingerprint [29], of physical devices, which can be used for security applications.

A PUF is a black-box function  $F(\cdot)$  which provides a unique and unclonable output, the *response*  $R = F(C)$ , given as input the *challenge*  $C$ . We refer to the pair  $C$  and  $R$  as the challenge-response pair (CPR). Figure 4 sketches how two different PUFs A and B (with functions  $F_A(\cdot)$  and  $F_B(\cdot)$ ) respond to two different challenges  $C_1$  and  $C_2$ . On the one hand, given two different

challenges  $C_1$  and  $C_2$ , the responses of the same PUF A,  $F_A(C_1)$  and  $F_A(C_2)$ , are different. On the other hand, the same challenge  $C_2$  provides two different responses  $F_A(C_2)$  and  $F_B(C_2)$ , when using two different PUFs.

Soft PUFs are used for PUFs with limited number of challenges, while strong PUFs are used for PUFs with a large number of challenges. In the latter case, the complete determination of the CRP is not possible in a feasible amount of time. The property of uniqueness is defined by means of the inter-Hamming distance of the outputs, that is how different are the responses of distinct PUFs. The reliability of a PUF is the ability to provide the same response for a given challenge; this is measured by the intra- Hamming distance, which is the HD among two responses to the same challenge and should ideally be equal to zero; while steadiness indicates the variability of the response due to changes in the circumstances e.g., temperature, power supply or aging effect [30].

Different kinds of PUFs exist, some of which are described in the following. The system presented in [31] is one of the first examples of a strong optical PUF. In this case, an input laser beam is directed towards a stationary scattering medium and then the speckle output pattern is recorded. The laser XY location and its polarization constitute the challenge while the response is the associated speckle pattern. Such a pattern is strongly dependent on the input location/polarization due to the fact that multiple scattering events can occur inside the scattering medium. Conversely, the power-on state of a static random access memory (SRAM) is a soft PUF. In fact, though an SRAM cell is symmetric, manufacturing anomalies can induce a tendency toward a logical “1” or “0” when the power is switched on. This variability is random across the entire SRAM and this determines a univocal fingerprint that can provide a distinctiveness. Another interesting example of soft PUF is obtained in the case of digital image (video) acquisition. When a photo is acquired, the camera sensor, which is composed of a two-dimensional array of charge coupled devices (CCDs), is hit by light photons and this energy is then converted into electron charges. Due to manufacturing imperfections, each cell of such a silicon sensor differently answers to a uniform incoming light. Consequently, this results in the superimposition, in each content it takes (images and/or videos), of a systematic noise, named photo response non-uniformity noise (PRNU) [32]. The PRNU is not perceivable and does not degrade the visual quality of the acquired contents, but it constitutes a fingerprint that is embedded within the image pixels. Such a fingerprint can be successively extracted by means of a filtering operation and compared with the reference fingerprints of different cameras to perform a source identification.

Overall, it is evident that PUFs have strong characteristics that can be used for optical identification (OI). For example, PUFs can be used for authentication purposes, by storing a database of CRPs ( $C_i, R_i$ ). Furthermore, PUFs can be used as a cryptographic root key for a device, such that key injection is not required, and the key cannot be copied and does not need to be stored but is simply recovered from the device when necessary.

However, despite the advantages, PUFs are anyway prone to security issues and should be carefully tackled in relation to the application scenario.

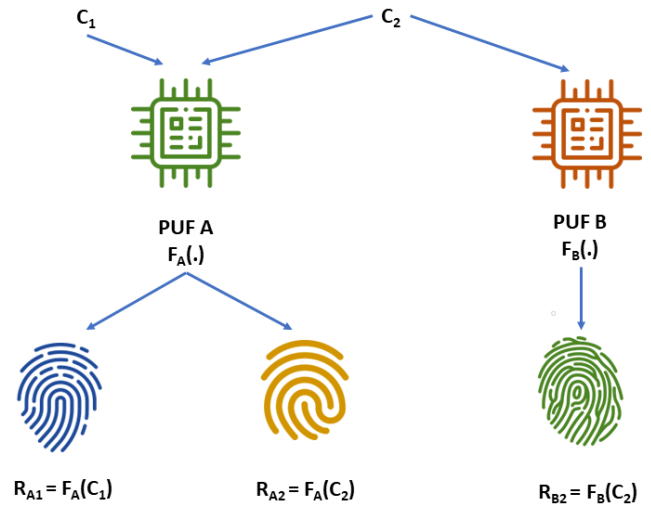


Fig. 4 Challenge-response pairs (CRPs) protocol.

## B. Rayleigh backscattering as an OPUF

The Rayleigh backscattering that occurs when stimulating optical fibers with propagating light is an OPUF, due to the random density fluctuations caused by the fabrication process [26]. Therefore, we propose to use the Rayleigh backscattering pattern (RBP) as a signature of the optical fiber, which allows us not only to identify the fiber link but any optical and opto-electronic sub-systems through their pigtail.

RPB acquisition can be done using the optical frequency domain reflectometry (OFDR) technique with sub-millimeter-level spatial resolution [32-36]. In this work, we consider the coherent OFDR (C-OFDR) since it allows us to increase the sensitivity and resolution [37,40].

C-OFDR is implemented as follows. The light from a continuous wave (CW) laser with amplitude  $E_0$ , whose frequency is linearly swept in time with sweep rate  $\gamma$ , propagates into the fiber under test (FUT). The RBP is the photocurrent obtained after self-coherent balance detection, as sketched in Figure 5, and can be modeled as

$$I(t) = E_0 \sum_{k=1}^n \sqrt{R_k} \cos(2\pi\gamma t \tau_k) \quad (5)$$

when there are  $n$  reflection points with reflectivity  $R_k$  and roundtrip time  $\tau_k$  [26,40].

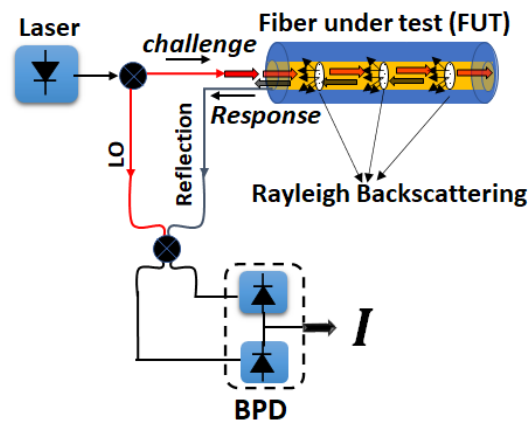


Fig. 5. RBP acquisition with C-OFDR. LO: local oscillator. BPD: Balanced photodetector.



## 4. POTENTIAL APPLICATIONS

### A. Physical layer security in classical communications

In this section, the possibilities and challenges of optical identification (OI) – or more in general of fingerprints – are discussed. The RBP of an optical fiber is an OPUF, and, therefore, each fiber can be characterized by a fingerprint. This fingerprint can be obtained, for example, offline before the fiber installation, having access to an end of the fiber. Let us assume that the operator maintains a database with the fingerprints of all fibers in the network, thus having awareness of all installed fibers. In this way, unauthorized access to the network can be revealed. In particular, potential applications are the identification of tampering (consisting of making fake nodes) or jamming (introducing harmful signals in the network). Indeed, fibers – e.g., attached to an edge port – can be checked and “authorized” periodically or on-demand according to management policies. Additional possibilities include also the extension of OPUF and fingerprint to other devices besides optical fibers (e.g., wavelength-selective switches), to directly identify also other devices.

Finally, a relevant issue related to amplifiers is here discussed. Amplifiers typically include isolators that limit the propagation of the signal-stimulating RBP. Thus, because of isolators, it is not possible to measure the fingerprint of a concatenation of fiber spans. Such an issue mainly impacts applications to backbone or metro networks, where amplifiers are typically employed. This may prevent an operator to limit the number of monitoring points for authentication. Indeed, if estimating the fingerprint of a concatenation of fibers from the knowledge of each fiber fingerprint would be possible, this could be checked against its measurement on the field identifying an intrusion in a point in between, without checking span by span. Differently, in a short-reach scenario, such as intra-data center or PONs where amplifiers are typically not needed, estimating the fingerprint of a concatenation of fibers can be very useful. Thus, this can pave the way for the study of models estimating the fingerprint of concatenated fibers. At the moment only preliminary works have been done on fingerprint concatenation [41,42] and more detailed studies are needed.

Another relevant challenge can be the automation of authentication and identification procedures relying on OPUF with the proposal of properly designed protocols, initiating the authentication procedure, disseminating measured fingerprints, correlating such measurements, and sending possible alarms when detecting intrusions.

### B. User authentication in quantum system

Since the term PUF was coined by Pappu et al. in 2001 [43], these objects gained a lot of interest and started to be used for a wide series of different security purposes such as identification and authentication, with applications in tamper evidence, anti-counterfeiting, etc. They have recently been adopted to face the authentication problem in quantum key distribution systems [44].

A generic QKD protocol is able to offer information-theoretically security (ITS) and its aim is to allow two users to establish a common secret key despite the presence of powerful adversaries. In order to succeed in this, two users employ a quantum channel that is thought to be open to possible tampering by an eavesdropper and a classical one which, instead, needs to be authenticated. Under these assumptions, an attacker can manipulate the raw key created via the exchange of the quantum states and only listen to the conversation over the classical channel. Here, with respect to classical protocols (symmetric and asymmetric classic cryptographic schemes), the laws of quantum mechanics provide the possibility to estimate a possible eavesdropper’s

intervention and the potential amount of information in her hands, so that the protocol can be eventually stopped [45]. This evaluation happens during the post-processing stage, performed along the classical channel: in this scenario, it appears of absolute importance a proper authentication of the classical channel, as each of the two legitimate parties of the conversation needs to rely on the other’s true identity in order to prevent a possible man-in-the-middle attack. In fact, a malevolent party, says Eve, can connect her QKD devices to the loose ends of the channels in order to hide her presence (Figure 6) so that she pretends to be Bob to Alice and Alice to Bob, modifying any message sent from Alice to Bob or vice versa.

The tool for this authentication job is the so-called message authentication code (MAC), for whose realization the Wegman-Carter authentication scheme and variations thereof are the most implemented methods; the security of this technique relies on mathematical complexity, as the probability of forgery is considered neglectable for polynomial-time adversaries [46]. Anyway, this kind of authentication requires a pre-shared key, which is usually considered the main drawback of QKD protocols; moreover, the need for a pre-shared secret key complicates considerably the design of large full-mesh QKD networks, as the number of keys has a quadratic growth with the number of users participating. In the past, different efforts were made to decrease the length of the pre-shared key in existing QKD protocols and to make easier their distribution and management [47].

A possible solution to this problem is the integration of the PUFs at the endpoints of the classical channel of a QKD apparatus, using their response as the tag generation required for the classical channel authentication. In particular, PUFs produce a random numerical key as a response to an input stimulus (called challenge), acting then as a pseudo-random number generator (PRNG). This tag is characterized by internal random disorder because the response to a given challenge reflects the internal disorder of the device: in this way, the response of a PUF can play the role of a fingerprint [48,49].

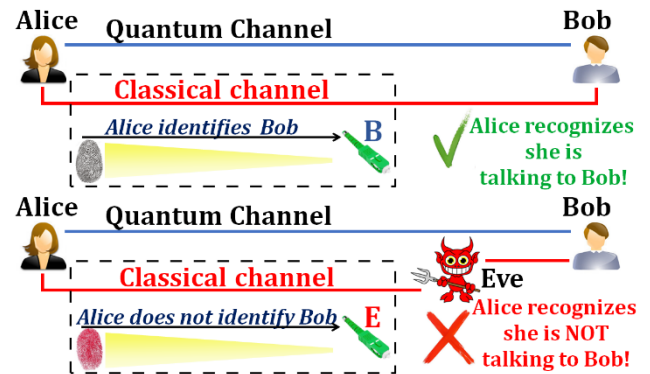


Fig.6. Schematic representation of the proposed authentication protocol: Alice can recognize whom she is talking with thanks to the Rayleigh light backscattered from the other’s party pigtail, as this provides a unique and unplayable fingerprint of her interlocutor.

Due to the unpredictable feature of PUFs, their use adds another layer of security in a QKD apparatus, as ITS is ensured under limited assumptions related mainly to the performance of the PUFs involved. The existing PUFs collections are so extensive that every class of them is characterized by features that can be useful concerning some applications. While Nikolopoulos [49] has considered the PUF tag, which is fabricated and attached to each QKD box (sender or receiver), we introduce here an OPUF, which is already present in the QKD box without manufacturing requirements and is an inherent feature of the QKD box, that eliminates such PUF tag disadvantages as tag scratching or stealing, or copying by adversaries, who have access to the PUF tag.

Considering that each QKD box includes the optical fiber (fiber optic transceiver pigtails), each QKD box can be uniquely identified by its ID generated by our proposed OPUF-based identification model, which is the RBP of its fiber optic pigtails. In this way, each QKD box carries the tag inside itself, i.e., its ID, which is hidden from the rivals, and just only the one that can measure it can observe the ID, whereas the external tag ID can be observed and copied by the adversaries. In summary, our proposed model is based on strong OPUF and seems a promising candidate for the authentication problem in the QKD system, which is also compatible with QKD infrastructures.

## 5. PRACTICAL OI APPLICATIONS IN OPTICAL COMMUNICATION SYSTEMS AND NETWORKS

In optical communication systems or networks, OI can be implemented through the measure of the RBP of the device pigtail or of the fiber link. Below we describe some implementation examples.

### A. Sub-system identification

Let us consider an optical sub-system having its own fiber pigtail whose length is generally in the order of 50-100 cm, which we use for RBP measure.

We consider a simulation scenario with a 0.5m fiber pigtail, and we measure the RBP with the C-OFDR with a sweep time 0.5, as in section 2. The analog signal is digitized using a single-bit analog to digital converter (ADC) with  $N = 4000$  samples.

Next, we convert the binary signature into a two-dimensional (2D) binary image, a QR code, comprising  $64 \times 64$  pixels, as shown in Figure 7. A key of 96 bits is added to obtain  $64 \times 64$  pixels and add an additional level of security to the system (since both the measure and key are needed for correct identification). The 2D QR consists of 64 rows, let us denote the length of each row as  $n = 64$ , and the matrix dimension as  $n^2$ .

Firstly, we investigate the robustness of the signature against brute force trials (BFT) by evaluating its inner-Hamming distance. Comparing all possible combinations of the 64 rows (which provides  $2016 = \binom{64}{2}$  pairs), we obtain 2016 HD values, ranging from 0 to  $n = 64$ . If the inner HD is too small or too large, it means that the rows are correlated, and one can be easily obtained from the other one. Conversely, it is desirable to have inner HD in average close to  $n/2 = 32$ . In our case, the histogram of the inner HD, shown in Figure 7(c), has a mean value of 31.9, very close to the optimal value.

Next, to assess the reproducibility and uniqueness of the signature, we consider the intra-Hamming and inter-Hamming distances, respectively. We generated 100 different signatures of the same sub-system, adding some random white Gaussian noise (in a practical system, repeated measurements are subject to noise). It is desirable that the HD of these signatures, the intra HD, is small, which indicates that the signature match is more probable. We also generated 100 different signatures representing 100 subsystems. Conversely, it is desirable that the HD among the signatures of different subsystems, the inter HD, is close to  $n^2/2$ , to ensure that it is difficult to match by mistake. Figure 8 (a) and (b) show the intra and inter-HD obtained by our simulations. The first has a mean value of 144.06, while the second a mean value of 1994.08, both showing excellent values.

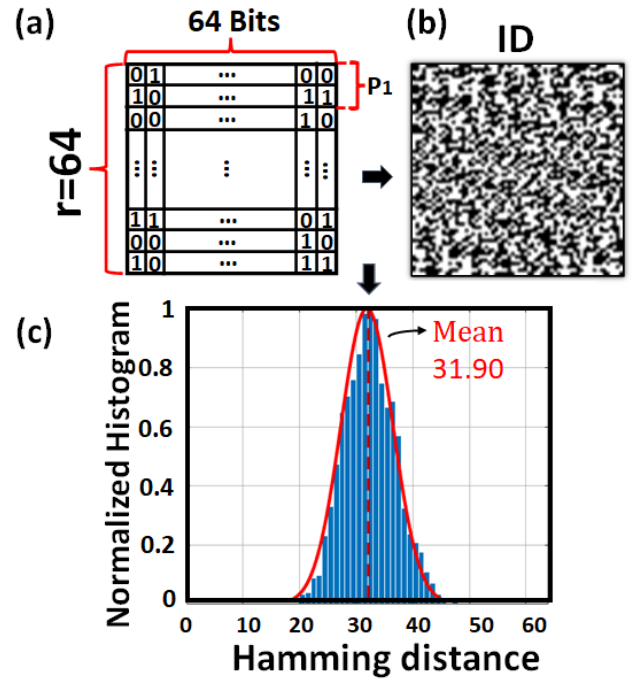


Fig. 7. Validation of the ID robustness against BFT attacks. (a) 2D binary ID data consists of  $64 \times 64$  bits. (b) The QR code. (c) Histogram (and Gaussian fit) of the inner-Hamming distance between the 2016 pairs of its 64 rows.

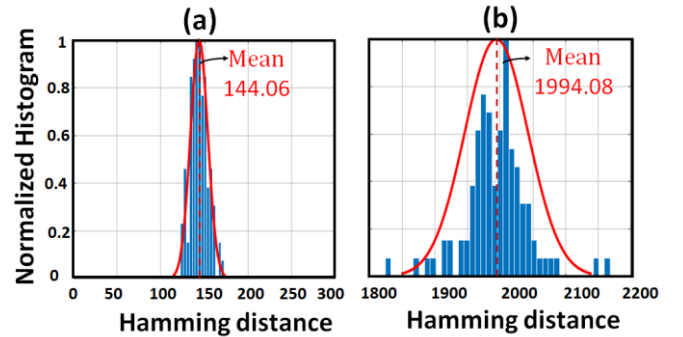


Fig. 8. Histogram of simulated 100 IDs for repeating the testing. (a) Intra-Hamming distance of one sub-system with 100 times measurements, shows ID reproducibility. (b) Inter-Hamming distance of 100 different IDs stored in the CRP database and one ID, which was not stored in the library, shows ID uniqueness.

We show in Figure 9 how the probability of false negative and false positive changes when the threshold changes. When  $\gamma$ , as defined in equation (2), approaches zero (one, respectively), the probability of false negative and false positive becomes 0.5 (minimum, respectively), while the probability of false positive becomes minimum (0.5, respectively). For  $\gamma = 0.5$  and SNR = 0 dB, the probability of false identification can be estimated to be in the order of  $10^{-60}$ .

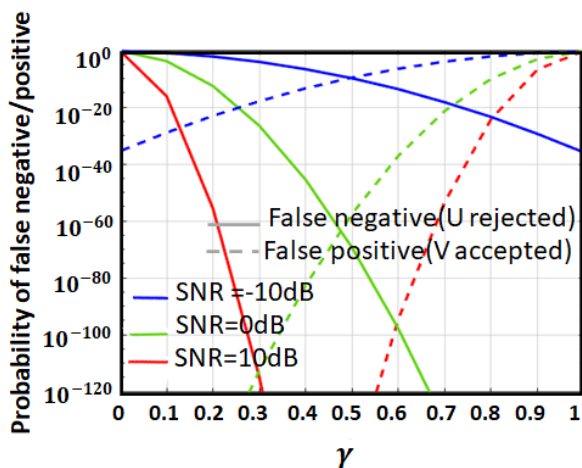


Fig. 9. Probability of false positive and negative as a function of  $\gamma$  for different SNR values.

## B. Path identification in optical networks

Let us consider the application of OI to an optical network. First, we take into account the simple case of two sub-systems (e.g., two optical fiber spans), then we extend our method to a large number of sub-systems in the network. Finally, two examples are considered for specific network topologies: point-to-point in the access segment, and point-to-point in the metro/core infrastructure.

### B.1 ID generation for two sub-systems

C-OFDR allows to measure RBPs provided by a single fiber/pigtail or a fiber concatenation. In optical networks, different fiber spans as well as passive sub-systems are plugged through fiber connectors which cause reflections due to the fiber-air interfaces. Such reflections appear as high back-reflected intensity peaks at each specific distance thus giving information about the link composition within the network. A typical reflectivity as a function of the distance including Rayleigh backscattering (RB) and connectors is shown in Figure 10. In the figure, an arbitrary fiber segment is identified for each fiber span through red and blue points respectively.

Network path identification is based on the measure and identification of the two concatenated fiber span signatures provided by segments RBPs. The procedure is detailed hereafter.

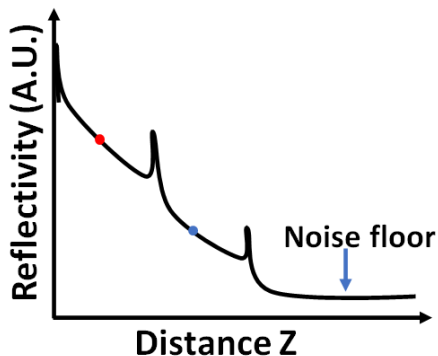


Fig.10 Backscattering typical reflection profile measured across three fiber connectors (peaks) and two fiber spans. Red and blue dots are chosen for fiber identification.

First, the RBPs associated to each fiber are measured through C-OFDR, and acquired with ADC. Next, a scanning window is applied to the RBP of each fiber to select a specific fiber subsection long enough to uniquely identify the fiber. We here take 26 cm for each fiber at the arbitrary distance shown in Figure 10 as red and blue points respectively. RBPs amplitudes are normalized to their maximum values. Figure 11 (top) shows the measured RBPs for the two fibers at the red (left) and blue (right) positions as described in Figure 10. For each RBP a reduced set of data  $S_1, S_2$  is selected for each fiber (red and blue color in the pictures respectively). For single fiber identification  $S_1$  and  $S_2$  can be quantized as described in the previous section. In the case of path identification, however,  $S_1$  and  $S_2$  are independently interpolated and overlapped in the distance domain to calculate the intersection points as shown in Figure 11 (bottom). Finally, points are transformed to the binary domain and converted to a QR code adding a binary random generated key as described in section A. The QR code represents the specific ID of the considered network path. Both the key and the ID are stored in a database and can be used for path identification through cross-correlation with reference IDs. If an adversary is able to physically access the network and measure each fiber RBPs, the identification is protected by the described encoding process.

For the performance evaluation of the proposed method, 200 independent network IDs (QR) are generated and stored into the database together with the related keys. Thus, the *challenge* is the sweeping parameters to measure the RBP, and the *response* is the binary image obtained from the RBP of the selected part of the fibers in the networks. Additionally, 25 fake IDs are randomly generated for testing purposes. After cross-correlation, none of the fake 25 IDs are identified as belonging to the database, and only genuine 200 IDs give positive response each having a single match.

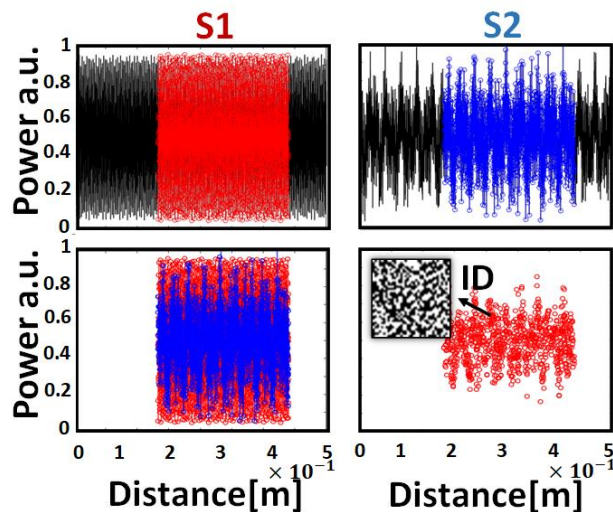


Fig. 11. Top: Selected backscattered data for the two fibers (left and right); bottom: (left) data superimposition, (right) intersection points and binary image (QR) as network ID.

### B.2 ID generation for cascaded sub-systems

ID generation is here described for a system including three devices (fibers) but can be extended to any number of sub-systems. In a first approach, we overlap the independent interpolations of selected data  $S_1, S_2$  measured for two fibers taking intersection points. These points are then treated as a new measure that is interpolated and overlapped to the next fiber measured data  $S_3$  as shown in Figure 12 (a). The



approach can be extended to a large number of fibers. The binary ID is, now, distilled by digitizing the intersection data provided by the last step. QR is obtained by adding a randomly generated binary sequence key  $k_1$ . As in the case of two fibers, QR and  $k_1$  are stored in the network database  $D_1$ .

Alternatively, the three-fiber ID may be obtained by cascading two independent IDs each distilled by digitizing the intersection data of two couple of fibers (e.g., 1, 2 & 2, 3), having length  $N_1$  and  $N_2$ , respectively. The resulting ID with length  $N_1 + N_2$  is obtained by IDs concatenation as shown in Figure 12 (b). A subset of the ID bits with length  $k_2$  is arbitrarily selected around the concatenation point so that  $k_2 \leq N_1 + N_2$ . In this case the choice of  $k_2$  is unknown to any adversary. The new obtained ID is finally transformed to a QR by adding a random generate binary sequence key  $k_1$  like in the previous case. Finally, QR is obtained by adding a randomly generated binary sequence key  $k_1$  and stored into the network database  $D_2$  (Figure 12 (b)).

Each approach is able to generate QRs of various sizes, which could be an additional challenge for adversaries. The same methods apply to any number of sub-systems over different optical network architectures.

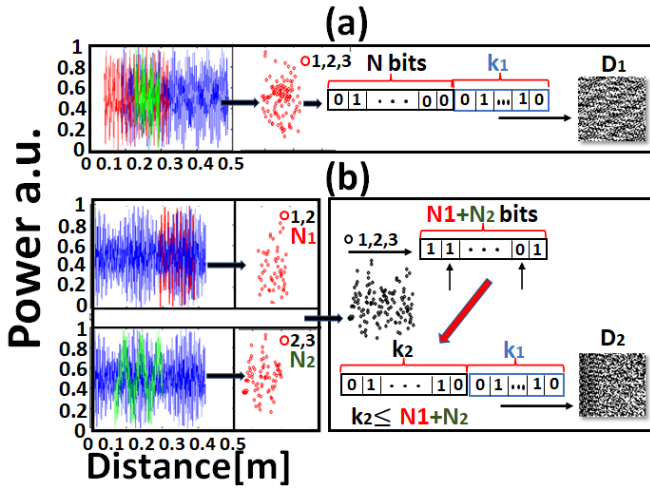


Fig. 12. Methods for the identification of a three-span link using (a) superimposition of three fibers, (b) concatenation of two couple of fibers' IDs.

### B.3 Point-to-point identification in the access segment

In an optical network, if the transmitter (Tx) and/or receiver (Rx) are able to perform RBP measurement, the identification will be implemented through direct measurement and cross-correlation. In an access network architecture as shown in Figure 13, the central node (CN) communicates point-to-point (P2P) with any connected user. The proposed technique allows to have mutual identification between CN and users if both have access to the database where ID are stored. In Figure 13 an identification example is shown. The CN sends challenge  $C_1$  through the fiber link to the user with  $ID_1$  and collects back response  $R_1$  represented by the RBP in black in the figure. A subset of the data is extracted (blue curve), sampled (red curve) and digitized to obtain the ID (QR). The CN, in this case, searches for ID into the database, and, if it finds a matching, it confirms user identification. A symmetric procedure is adopted by the user for CN identification.

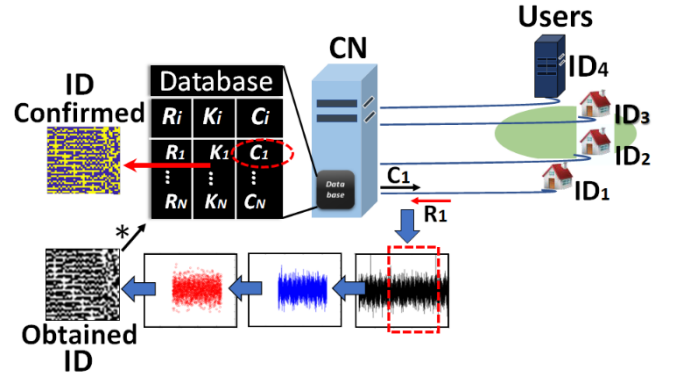


Fig. 13. User  $ID_1$  identification procedure by central node (CN) in a P2P architecture.

### B.4 Point-to-point identification in the metro/core infrastructure

In metro and core optical networks, where paths may overcome 50km length, RBP measures can be very noisy or not feasible due to the fiber attenuation. We propose here a central node (CN)-assisted identification strategy for long distances exploiting RBP detailed in Figure 14. Two ID databases  $D_1, D_2$  are generated using two different keys  $k_1, k_2$ . The CN communicates to the user a specific challenge  $C_1$  that the user must send for link identification measure in the proximity of his site (fiber pigtail of last mile fiber). The response  $R_1$  is collected by the user as the RBP and it is coded using one of the two keys arbitrarily (e.g.,  $k_1$ ). The obtained ID is sent to the CN who search for a match into both  $D_1$  and  $D_2$ . If the CN finds the ID into one of the two databases, it asks the user which of the two keys he did use. If the key corresponds to the database where match was found, ID is confirmed. In this way, the access to the link by an adversary that may read the RBP, is not enough for the identification process that is protected by the knowledge of the used key.

In contrast to the traditional PUF challenge-response database, in which any single challenge ends with a response, in the proposed method, each challenge can be used for several fibers. That is, one challenge could be used for several fibers providing different responses. This method also reduces the OPUF challenge-response database size.

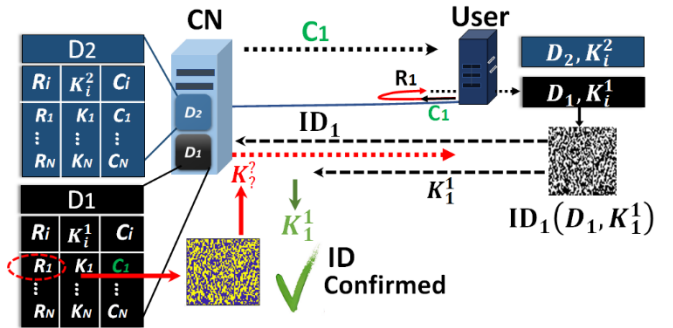


Fig. 14. Central node (CN) assisted user identification in a metro/core infrastructure.

## 6. CONCLUSION

In this work, we have proposed for the first time the concept of optical identification (OI) for network security purposes at the physical layer. In particular, we propose to use the fingerprint of each network's sub-system to identify, authenticate, and monitor an optical network. We



introduce the concept of OI and we describe a technique to assess the identification reliability. Next, we propose to use the physical unclonable functions (PUFs) for OI, to exploit the intrinsic unclonability and uniqueness of PUFs. In particular, we propose to use the Rayleigh backscattering, an optical PUF, to identify a fiber. In this way, each sub-system of a network can be identified just using its pigtail (or the fiber itself for a link), without any additional device, and working directly at the physical layer. To highlight the huge possibilities of this technique and its potential impact in the field, we described two possible applications of OI: physical layer security in classical communications and user authentication in QKD. On the one hand, we highlighted how OI at the physical layer can significantly enhance the security of an optical network through the identification of sub-systems and links. On the other hand, we described how OI can be effectively used for the authentication of the users (Alice and Bob) in a QKD system. Indeed, the authentication of the users (sometimes referred to as authentication of the classical channel) before QKD transmission is essential to ensure the reliability of the whole process and is usually done with conventional cryptographic methods (e.g., the MAC).

We described, as practical OI applications in optical communication systems and networks, how OI can be implemented for the identification of a fiber or a fiber pigtail in a point-to-point scenario and for the identification of a path in an optical network with passive components.

The OI concept represents an innovative approach to physical layer security which can be applied to any optical communication system and network. OI is based on existing intrinsic characteristics of physical sub-systems and it provides additional features to optical systems and networks operation.

**Funding Information.** HORIZON-JU-RIA (101096909), HORIZON-RIA (101092766), EU – NGEU (PE00000014).

## References

1. A. D. Wyner, "The wire-tap channel," in *The Bell System Technical Journal*, vol. 54, no. 8, pp. 1355-1387, Oct. 1975, doi: 10.1002/j.1538-7305.1975.tb02040.
2. X. Zhou and M. R. McKay, "Secure Transmission With Artificial Noise Over Fading Channels: Achievable Rate and Optimal Power Allocation," in *IEEE Transactions on Vehicular Technology*, vol. 59, no. 8, pp. 3831-3842, Oct. 2010, doi: 10.1109/TVT.2010.2059057.
3. M. Bloch and J. Barros, "Physical-Layer Security: From Information Theory to Security Engineering," Cambridge, U.K.: Cambridge Univ. Press, 2011.
4. Eyal Wohlgenuth, Yaron Yoffe, Pantea Nadimi Goki, Muhammad Imran, Francesco Fresi, Prajwal Doddaballapura Lakshmiyasimha, Roi Cohen, Prince Anandarajah, Luca Poti, and Dan Sadot, "Stealth and secured optical coherent transmission using a gain switched frequency comb and multi-homodyne coherent detection," *Opt. Express* 29, 40462-40480 (2021).
5. C. Gidney and M. Eker, "How to factor 2048-bit RSA integers in 8 hours using 20 million noisy qubits," *Quantum*, vol. 5, p. 433, 2021.
6. C. H. Bennett and G. Brassard, "Quantum cryptography: Public key distribution and coin tossing," in *Proc. IEEE Int. Conf. Computers, Systems, and Signal Processing*. New York: IEEE Press, 1984, p. 175.
7. Cavaliere F., Prati E., Poti L., Muhammad I., Catuogno T., "Secure quantum communication technologies and systems: from labs to markets," *Quantum Reports*, vol. 2, n. 1, pp. 80-106, 2020.
8. J. He, R. Giddings, W. Jin and J. Tang, "DSP-Based Physical Layer Security for Coherent Optical Communication Systems," in *IEEE Photonics Journal*, vol. 14, no. 5, pp. 1-11, Oct. 2022, Art no.7250611, doi: 10.1109/JPHOT.2022.3202433.
9. B. Wu, Z. Wang, Y. Tian, M.P. Fok, B.J. Shastri, D.R. Kanoff, P.R. Prucnal, "Optical Steganography Based on Amplified spontaneous emission noise," *Opt. Express* 21 (2) (2013) 2065–2071.
10. E. Wohlgenuth et al., "A Field Trial of Multi-Homodyne Coherent Detection over Multi-Core Fiber for Encryption and Steganography," in *Journal of Lightwave Technology*, doi: 10.1109/JLT.2023.3237249.
11. Haripriya Rout, Brojo Kishore Mishra, Pros and Cons of Cryptography, Steganography and Perturbation techniques, *IOSR J. Electron. Commun. Eng.* (2014) 76–81.
12. Rina Mishra, Praveen Bhanodiya, A review on steganography and cryptography, in: 2015 International Conference on Advances in Computer Engineering and Applications, IEEE, 2015, pp. 119–122.
13. Longsheng Wang, Xiaoxin Mao, Anbang Wang, Yuncai Wang, Zhensen Gao, Songsui Li, and Lianshan Yan, "Scheme of coherent optical chaos communication," *Opt. Lett.* 45, 4762-4765 (2020)
14. Piotr Antonik, Marvyn Gulina, Jaël Pauwels, Damien Rontani, Marc Haelterman, et al., "Spying on chaos-based cryptosystems with reservoir computing," 2018 International Joint Conference on Neural Networks, IJCNN 2018, Jul 2018, Rio de Janeiro, Brazil. pp.8489102, 10.1109/IJCNN.2018.8489102.hal-02432576
15. Wenhui Chen and Penghua Mu, 'Research on methods of enhancing physical layer security of optical fiber communication system in the smart grid', 2022 J. Phys.: Conf. Ser. 2237 012002
16. Jiang N, Zhao A, Liu S, et al. (2020) Injection-locking chaos synchronization and communication in closed-loop semiconductor lasers subject to phase-conjugate feedback. *Optics express*, 28(7): 9477-9486.
17. Mahdi Shakiba-Herfeh, Arsenia Chorti, H. Vincent Poor. 'Physical Layer Security: Authentication, Integrity and Confidentiality'. *Physical layer security and wireless secrecy*, Springer Nature, 2020.
18. E. Peterson, "Developing tamper-resistant designs with zynq ultrascalep devices (XAPP1323)," Xilinx, 2017.
19. L. Zhang, X. Fong, C. Chang, Z. H. Kong, and K. Roy, "Highly reliable memory-based physical unclonable function using spin-transfer torque MRAM," in *Proceedings of IEEE International Symposium on Circuits and Systems (ISCAS)* (2014), pp. 2169–2172.
20. Rührmair U., Devadas S. & Koushanfar F. Security Based on Physical Unclonability and Disorder. In *Introduction to Hardware Security and Trust* (eds. Tehranipoor, M. & Wang, C.) 65–102 (Springer, 2012).
21. Uppu, R. et al. Asymmetric cryptography with physical unclonable keys. *Quantum Sci. Technol.* 4, 045011 (2019).
22. Mesaritakis, C. et al. Physical unclonable function based on a multi-mode optical waveguide. *Sci. Rep.* 8, 1–12 (2018).
23. Goorden, S. A., Horstmann, M., Mosk, A. P., Škorić, B. & Pinske, P. Quantum-secure authentication of a physical unclonable key. *Optica* 1, 421–424 (2014).
24. Horstmeyer, R., Judkewitz, B., Vellekoop, I. M., Assaworarith, S. & Yang, C. Physical key-protected one-time pad. *Sci. Rep.* 3, 3543(2013).
25. F.Pavanello, I. O'Connor, U. Rührmair, A.C.Foster, D.Syridis, "Recent Advances in Photonic Physical Unclonable Functions," IEEE European Test Symposium (ETS), pp.1-10, May 2021[26th IEEE European Test Symposium (ETS), Bruges, Belgium, 2021]. DOI:10.1109/ETS50041.2021.9465434.
26. Y. Du, S. Jothibas, Y. Zhuang, C. Zhu and J. Huang, "Unclonable Optical Fiber Identification Based on Rayleigh Backscattering Signatures," *J. Light. Technol.*, vol. 35, no. 21, pp4634-4640, 2017, DOI: 10.1109/JLT.2017.2754285
27. A. Wali, A. Dodda, Y. Wu, A. Pannone, L. K. Reddy Usthili, S. K. Ozdemir, I. T. Ozbolat, and S. Das, "Biological physically unclonable function," *J. Commun Phys*, 2019, vol. <https://doi.org/10.1038/s42005-019-0139-3>
28. C. Herder, M. -D. Yu, F. Koushanfar and S. Devadas, "Physical Unclonable Functions and Applications: A Tutorial," in *Proceedings of the IEEE*, vol. 102, no. 8, pp. 1126-1141, Aug. 2014, doi: 10.1109/JPROC.2014.2320516.

29. A. K. Jain, D. Deb and J. J. Engelsma, "Biometrics: Trust, But Verify," in IEEE Transactions on Biometrics, Behavior, and Identity Science, vol. 4, no. 3, pp. 303-323, July 2022, doi: 10.1109/TBIOM.2021.3115465.
30. J. Kong and F. Koushanfar, "Processor-Based Strong Physical Unclonable Functions With Aging-Based Response Tuning," in IEEE Transactions on Emerging Topics in Computing, vol. 2, no. 1, pp. 16-29, March 2014, doi: 10.1109/TETC.2013.2289385.
31. R. S. Pappu, P. S. Ravikanth, B. Recht, J. Taylor, and N. Gershenfeld, "Physical one-way functions," Science, vol. 297, pp. 2026-2030, 2002
32. M. Chen, J. Fridrich, M. Goljan and J. Lukas, "Determining Image Origin and Integrity Using Sensor Noise," in IEEE Transactions on Information Forensics and Security, vol. 3, no. 1, pp. 74-90, March 2008, doi: 10.1109/TIFS.2007.916285.
33. J. Clement, H. Maestre, G. Torregrosa, and C. R. Fernández-Pousa, "Incoherent Optical Frequency-Domain Reflectometry Based on Homodyne Electro-Optic Downconversion for Fiber-Optic Sensor Interrogation," Sensors, vol. 19, no. 9, p. 2075, May 2019, doi: 10.3390/s19092075.
34. Z. Ding et al., "Compensation of laser frequency tuning nonlinearity of a long range OFDR using Deskew filter," Opt. Exp., vol. 20, no. 3, pp. 3826-3834, Feb. 2013.
35. J. Song, W. Li, P. Lu, Y. Xu, L. Chen and X. Bao, "Long-Range High Spatial Resolution Distributed Temperature and Strain Sensing Based on Optical Frequency-Domain Reflectometry," in IEEE Photonics Journal, vol. 6, no. 3, pp. 1-8, June 2014, Art no. 6801408, doi: 10.1109/JPHOT.2014.2320742.
36. S. Zhao, J. Cui, L. Suo, Z. Wu, D. -P. Zhou and J. Tan, "Performance Investigation of OFDR Sensing System With a Wide Strain Measurement Range," in Journal of Lightwave Technology, vol. 37, no. 15, pp. 3721-3727, 1 Aug. 2019, doi: 10.1109/JLT.2019.2918379.
37. K. Tsuji, K. Shimizu, T. Horiguchi and Y. Koyamada, "Coherent optical frequency domain reflectometry for a long single-mode optical fiber using a coherent lightwave source and an external phase modulator," IEEE Photon. Technol. Lett., vol. 7, pp. 804-806, 1995.
38. K. Tsuji, K. Shimizu, T. Horiguchi and Y. Koyamada, "Coherent optical frequency domain reflectometry using phase-decorrelated reflected and reference lightwaves," in Journal of Lightwave Technology, vol. 15, no. 7, pp. 1102-1109, July 1997, doi: 10.1109/50.596955.
39. J. Geng, C. Spiegelberg, and S. Jiang, "Narrow linewidth fiber laser for 100 km optical frequency domain reflectometry," IEEE Photon. Technol. Lett., vol. 17, no. 9, pp. 1827-1829, Sep. 2005.
40. F. Ito, X. Fan, and Y. Koshiyaki, "Long-Range Coherent OFDR With Light Source Phase Noise Compensation [Invited]," J. Light. Technol., vol. 30, no. 8, pp. 1015-1024, 2012, DOI: 10.1109/JLT.2011.2167598
41. P. N. Goki, T. T. Mulugeta, N. Sambo, R. Caldelli and L. Poti, "Optical Network Authentication through Rayleigh Backscattering Fingerprints of the Composing Fibers," GLOBECOM 2022 - 2022 IEEE Global Communications Conference, Rio de Janeiro, Brazil, 2022, pp. 2146-2150, doi: 10.1109/GLOBECOM48099.2022.10001427.
42. P. N. Goki, T. T. Mulugeta, N. Sambo and L. Poti, "Network Authentication, Identification, and Secure Communication through Optical Physical Unclonable Function," 2022 European Conference on Optical Communication (ECOC), Basel, Switzerland, 2022, pp. 1-4.
43. R. Pappu, B., Recht, J. Taylor, & N. Gershenfeld, "Physical one-way functions." Science 297.5589 (2002): 2026-2030.
44. Skoric, B. "Quantum readout of physical unclonable functions: Remote authentication without trusted readers and authenticated quantum key exchange without initial shared secrets." Cryptology ePrint Archive (2009).
45. R. Alba Gaya, Antonio, et al. "Practical quantum key distribution based on the BB84 protocol." Waves. Vol. 1. No. 3. Instituto de Telecomunicaciones y Aplicaciones Multimedia (ITEAM), 2011.
46. Rosulek, Mike. 'The Joy of Cryptography OE (1st)', chapter 10: "Message Authentication Codes." (2017).
47. M. Peev, et al. "A novel protocol-authentication algorithm ruling out a man-in-the-middle attack in quantum cryptography." International Journal of Quantum Information 3.01 (2005): 225-231.
48. López Ríos, Blanca A. "Evaluation of PUF and QKD integration techniques as root of trust in communication systems." Chapter 3: Integration of PUFs into the BB84 protocol (2022).
49. Nikolopoulos, Georgios M., and Marc Fischlin. "Quantum key distribution with post-processing driven by physical unclonable functions." arXiv preprint arXiv:2302.07623 (2023).